Comparison of three SECT calibration methods to convert CT data to RSP values for biological tissues.

Bachelor thesis theoretical physics

Bas A. de Jong

Date: 24-6-2016

Supervisors: E.R. van der Graaf and A.K. Biegun.
Medical physics group KVI-CART, RUG, Groningen.

university of groningen

kvi - center for advanced radiation technology

1. Table of contents.

2. Introduction

In the Netherlands 105,000 people were diagnosed with cancer in 2015, and this number is increasing every year, as the average age of the population increases [Ci16]. Cancer is treated in many different ways, depending on the position, type and stadium of the cancer. One way of treating cancer is using radiotherapy. More than half of the people who suffer from cancer need radiotherapy to control the growth of tumours. In radiotherapy the tumour is irradiated with ionizing radiation. Different particles or modalities can be chosen to do this irradiation. The most common modality uses high energy photons, but electrons, protons, or other nuclei of small atoms can also be used. The Dutch board of health estimated that about 10% of the cancer patients in the Netherlands in 2015 could benefit from proton therapy. Currently there are Four initiatives for building proton therapy centres in the Netherlands, in Amsterdam, Maastricht, Delft and Groningen [PT16]. In Delft and Groningen they are already building the facilities. Groningen expects its first patients to be treated in 2017.

The advantage of proton therapy over the conventional photon therapy originates from the difference in dose delivered to the healthy tissue of the patient. Protons slow down inside the patient's body and come to a stop, therefore almost no dose is delivered to the healthy tissue behind the tumour. This is different from therapy using high energy photons. Photons can travel through the whole body resulting in a exponentially decreasing dose distribution. Furthermore, as the protons slow down they start to give of more energy to the tissue they are traveling through, resulting in a dose peak called the Bragg peak at the end of their trajectory. By using a superposition of dose distributions of proton beams with different proton kinetic energies it is possible to create a spread out Bragg peak (SOBP), which gives a uniform dose distribution over the tumour (Figure 1)[Pe16]. From inspection of Figure 1 it can be concluded that both in front as well as behind the tumour a lower dose is delivered to the healthy tissue using the SOBP, while delivering the same dose to the tumour, this shows the clear physical advantage proton therapy can have over photon therapy.

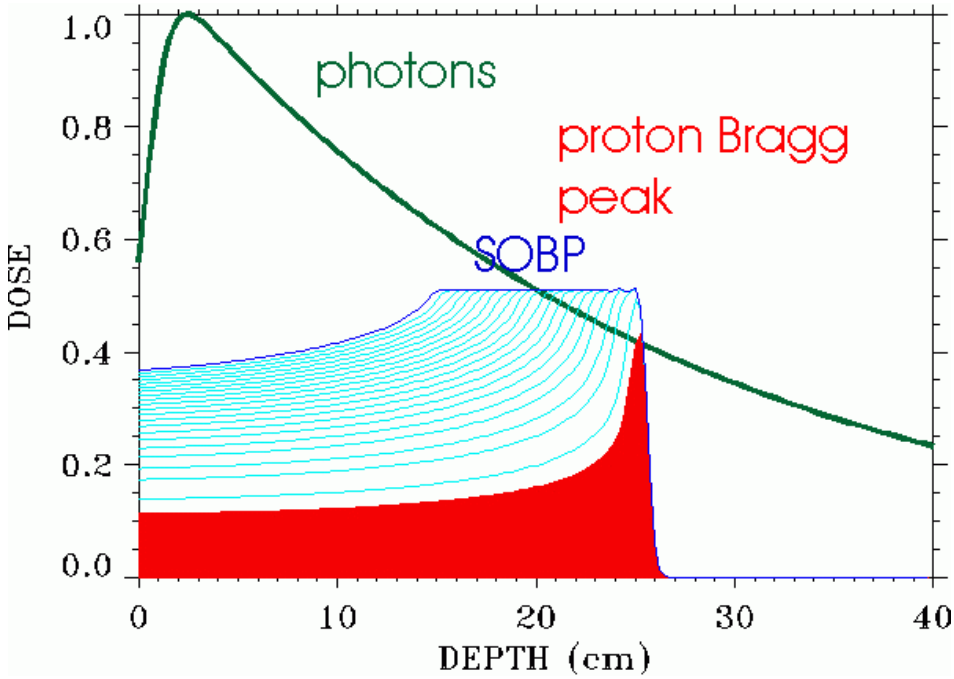

Figure 1: Plot of the dose distributions for irradiation using a single beam of photons and irradiation with protons as function of depth [Pe16].

Proton therapy in its current state of technology already is a valuable tool in the battle against cancer. But it is a technologically advanced technique, and there are still improvements to be made. For instance, in proton therapy it is important to know how far the protons will penetrate the body. If the range of the protons is over- or under estimated, damage will be done to healthy tissue surrounding the tumour or, the tumour might not get enough dose to be properly controlled. The proton ranges are estimated by calculating proton ranges from CT data. Currently a margin of typically 3-3.5% is used around the tumour to account for uncertainties in the estimated range of the protons [Ai14].

In this report we will consider, and compare three different single energy CT (SECT) calibration methods to convert CT scaled Hounsfield units to proton ranges expressed as relative stopping powers (RSP) for biological tissues. The different calibration methods are:

-The direct calibration method, in which a single linear relation is used convert CT scaled Hounsfield units to RSP values.

-The stoichiometric calibration method, in which a parameterized model for the response of the CT unit is calibrated, then this model is used to calculate scaled Hounsfield units for a larger set of biological tissues of which the compositions and RSP values are known. After this, calibration curves are fitted to these scaled Hounsfield units and RSP values for the tissues to interpolate RSP values for all CT data.

-The composition lookup table calibration method, in which CT scaled Hounsfield units are converted to density information by linear interpolation within a CT-to-density table thereafter a certain composition and mean ionisation potential from a composition lookup table is linked to the density. From the interpolated density together with the composition and ionization potential data RSP values are calculated.

3. Synthetic Hounsfield units and theoretical RSP values

In this report synthetic scaled Hounsfield units and theoretical RSP values are used evaluate RSP values and scaled Hounsfield units from the different calibration methods. The synthetic scaled Hounsfield units can be considered the Hounsfield units that would be measured on a CT scanner in which effects like hardening of the X-ray spectrum and disturbances from artefacts are perfectly corrected for. These effects are also not considered in the different calibration methods, so it is consistent to use the synthetic data comparisons. The synthetic and theoretical data can be calculated from material properties: elemental composition, density and elemental cross sections for photons, combined with information about the spectrum of a CT X-ray tube and CT detector efficiency.

3.1 Calculation of synthetic scaled Hounsfield units.

To calculate synthetic scaled Hounsfield units, first photon energy dependent attenuation coefficients $\mu_x(E)$ are calculated for compound x using material properties: density, elemental composition and photon cross sections for the elements [Ja81]:

$$\mu_x(E) = \rho_x N_A \sum_{i}^{All\ elements} \omega_i \frac{Z_i}{A_i} \cdot \frac{\sigma_{ai}(E)}{Z_i} \qquad [1]$$

in which:
ρ_x: the mass density of compound x;
$N_A = 6.022 \cdot 10^{23}\text{mol}^{-1}$: Avogadro's number;
ω_i: the mass fraction of elements i in compound x;
$\frac{Z_i}{A_i}$: the ratio between the atomic number and atomic weight of element i in compound x;
$\sigma_{ai}(E)$: atomic dependent photon cross section for element i.

In CT imaging a spectrum of photon energies from the X-ray tube is used to make the image. Detectors have different sensitivities for the different photon energies. The system weighting function describes both the X-ray spectrum and the energy dependent sensitivity of the detector of the CT scanner and gives the weights φ_j for discrete energies E_j in the spectrum, with j=1 2 . . N, the number of discrete energies in the spectrum. For which: $\sum_{j=1}^{N} \varphi_j = 1$. Using the energy dependent attenuation coefficients and the system weighting function of the CT scanner, the mean attenuation coefficient $\bar{\mu}_x$ for compound x is given by:

$$\bar{\mu}_x = \sum_{j=1}^{N} \varphi_j \cdot \mu_x(E_j) \qquad [2]$$

We introduce the scaled Hounsfield unit H, which is given by the following relationship:

$$H = \frac{\bar{\mu}_x}{\bar{\mu}_{H_2O}} \cdot 1000 \qquad [3]$$

In which $\bar{\mu}_{H_2O}$ and $\bar{\mu}_x$ are the mean attenuation coefficients for water and compound x respectively.

Synthetic Hounsfield units were calculated for 81 biological (human) tissues [Wh87], which are used for evaluation of the accuracy and precision of the calibration, and calculated for 15 tissue equivalent calibration materials [Ab16][Ni16][Table 1], which are used to perform the calibrations, using composition information of the materials together with NIST photon cross section data [Ni15] and the system weighting function of a Siemens Force 120 keV system weighting function [Si16] (Figure 2).

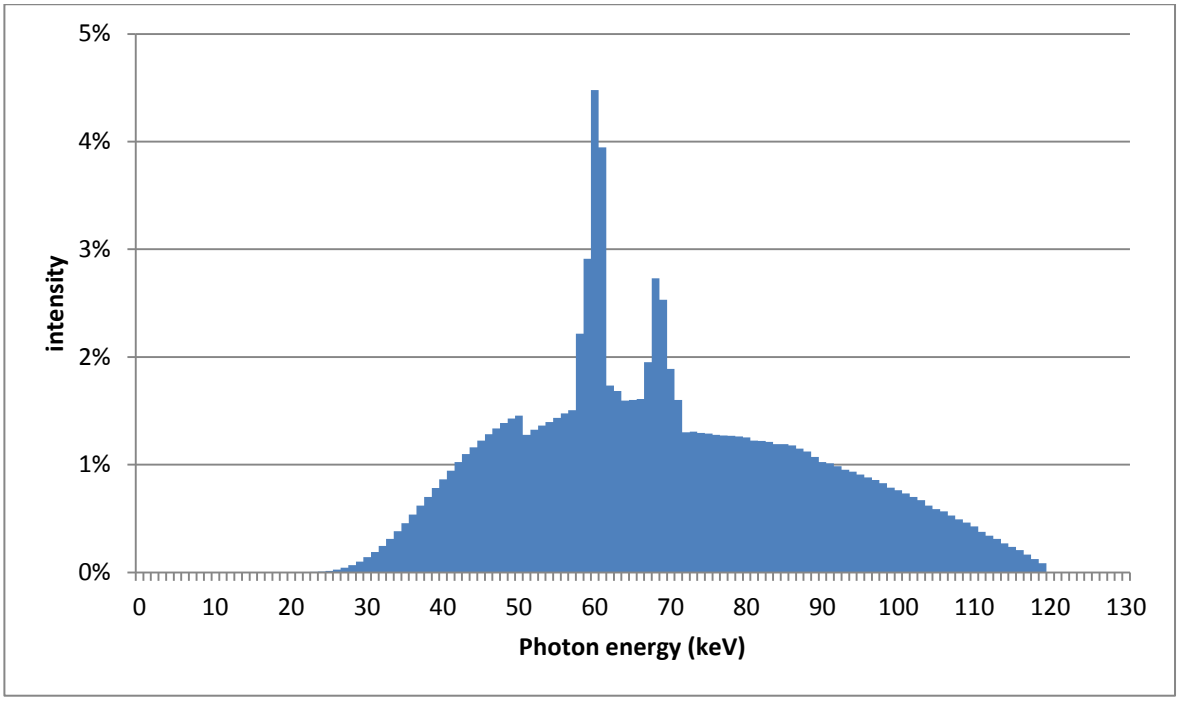

Figure 2: System weighting function with intensities per keV energy bin of a Siemens Force 120 keV CT scanner.

3.2 Calculation of mass stopping powers for elements

Theoretical relative stopping powers are calculated using the Bethe-Bloch equation. The Bethe-Bloch equation is a relativistic quantum mechanical formula, which predicts the linear energy transfer $-\frac{dE}{dx}$ of a charged particle to a uniform material, while it traverses this material. The mass stopping power is the linear stopping power divided by the mass density and is given by [Tu07]:

$$\frac{S}{\rho} = -\frac{1}{\rho}\frac{dE}{dx} = \frac{Z}{A}\frac{K}{M_u\beta^2}\left[\ln\frac{2m_e c^2\beta^2}{I(1-\beta^2)} - \beta^2\right] \qquad [4]$$

in which:
$\frac{S}{\rho} = -\frac{1}{\rho}\frac{dE}{dx}$: the mass stopping power (in MeV cm^2 g^{-1});
$K = 4\pi r_e^2 m_e c^2 N_A = 0.3070\ \text{MeV cm}^2\ \text{mol}^{-1}$: a constant;
$r_e = \frac{e^2}{4\pi\varepsilon_0 m_e c^2} = 2.818 \cdot 10^{-13}$ cm : the classical electron radius;
$e = 1.602 \cdot 10^{-19}$ C: the charge of the electron;
$m_e c^2 = 0.511$ MeV : the electron rest mass;
$\varepsilon_0 = 8.854 \cdot 10^{-12}\text{C}^2\text{N}^{-1}\text{m}^{-2}$: the permittivity of free space;
$M_u \equiv 1\text{g mol}^{-1}$: the molar mass constant;
β: the speed of the projectile relative to the speed of light;
I: the mean excitation energy of the target material in (MeV);
Z: the atomic number of the target material;
A: the atomic mass of the target material.

The speed of the projectile relative to the speed of light β depends on the kinetic energy of the proton. β^2 is calculated using the following equation:

$$\beta^2 = 1 - \frac{1}{\left(1 + \frac{E}{m_p c^2}\right)^2} \qquad [5]$$

in which:
$E = 100$ MeV: is the ''mean'' kinetic energy of the proton.
$m_e c^2 = (938.3$ MeV) is the proton rest mass.

If the energy dependency of the velocity cannot be taken into account, a kind of average kinetic energy for the protons should be chosen. Yang et al [Ya12] advocate a value of 100 MeV for the energy of the protons. Using equation [5] this results in a value for β^2 of 0.1833.

For all different elements i the mass stopping powers $\left(\frac{S}{\rho}\right)_i$ can now be calculated using equation [4]. For the calculation, the atomic number *Z*, atomic mass *A*, and the mean ionization potential of the element have to be used. In this report NIST Ionization potential data was used [Ni15].

3.3 Calculation of theoretical RSP values for compounds

The relative stopping powers for compounds can be calculated from the mass stopping powers for different elements and the composition of the compounds. An additional formula is needed to account for the composition of elements in the compounds. The formula used is the Bragg additivity rule. According to the Bragg additivity rule, the mass stopping power for compound x: $\left(\frac{S}{\rho}\right)_x$ can be calculated using a linear addition of the mass stopping power of the elements it is composed of [Pa12]:

$$\left(\frac{S}{\rho}\right)_x = \sum_i \omega_i \left(\frac{S}{\rho}\right)_i \quad [6]$$

in which $\left(\frac{S}{\rho}\right)_i$ is the mass stopping power and ω_i is the mass fraction of the different elements in the compound. Linear stopping powers for compounds are calculated by multiplying the mass stopping power with the mass density of the compound:

$$S_x = \left(\frac{S}{\rho}\right)_x \cdot \rho_x \quad [7]$$

The relative stopping power RSP is introduced as the ratio of the stopping power of compound x: S_x relative to the stopping power of water S_w:

$$\mathrm{RSP} = \frac{S_x}{S_{H_2O}} \quad [8]$$

Theoretical RSP values were calculated from the composition information of the 15 calibration materials which are given in Table 1, and the composition information of the 81 biological tissues.

Table 1: Synthetic scaled Hounsfield units and theoretical RSP values of the fifteen calibration materials.

Material	Synthetic H	Theoretical RSP
AIR	1	0.00
LN300	284	0.28
LN450	419	0.42
AP6	877	0.92
BR12	932	0.95
BRN-SR2	986	1.03
CT SW	996	0.98
water	1000	1.00
SW M4	1027	1.01
LV1	1077	1.06
IB3	1366	1.12
B200	1374	1.13
CB2-30%	1634	1.30
CB2-50%	2226	1.53
SB3	2910	1.79

4. The direct calibration method

The direct calibration method is one of the most straightforward ways of getting a calibration curve for converting CT scaled Hounsfield units to RSP values. In this method a limited number of calibration materials is used (in this study we will use 6), which have a well know composition. Scaled Hounsfield units are measured in the CT scanner (in this report synthetic scaled Hounsfield units are used for this). From the composition together with information about the mean ionization potential, RSP values are calculated for the calibration materials using the Bethe-Bloch equation and the Bragg additivity rule [Equations 4,5,6,7 and 8] like the theoretical RSP values. These RSP values are then plotted against the scaled Hounsfield units. A linear fit in this plot will then be the calibration curve.

4.1 The direct linear calibration curve

In performing the direct calibration method it is important to choose tissue equivalent calibration materials which span the whole scaled Hounsfield units scale. This allows for interpolation of RSP values for all Hounsfield units from the data acquisition instead of extrapolation, which is generally more uncertain. It is wise to choose calibration materials which are spread evenly between 0 < H < 3000, the domain to be expected from a real CT image. Furthermore, if the elemental composition of the calibration materials differs significantly compared with biological tissues the RSP of the material may also differ significantly, resulting in a poor calibration curve. The calibration materials which were used and corresponding synthetic scaled Hounsfield units and RSP values can be found in Table 2.

Table 2: Tissue equivalent calibration materials used for the direct calibration method, with corresponding scaled Hounsfield units and RSP values.

Material	RSP	H
LN300	0.283	284
AP6	0.915	877
SW M457	1.010	1027
CB2-30%	1.297	1634
CB2-50%	1.527	2226
SB3	1.792	2910

In a plot of the RSP values and the synthetic scaled Hounsfield units of the calibration materials a linear relation was fit using the least squares method (Figure 3). This resulted in a relation between RSP values and scaled Hounsfield units of: $\mathrm{RSP} = (5.3 \cdot 10^{-4} \pm 7 \cdot 10^{-5})H + (0.3 \pm 0.2)$. In which H is the scaled Hounsfield unit.

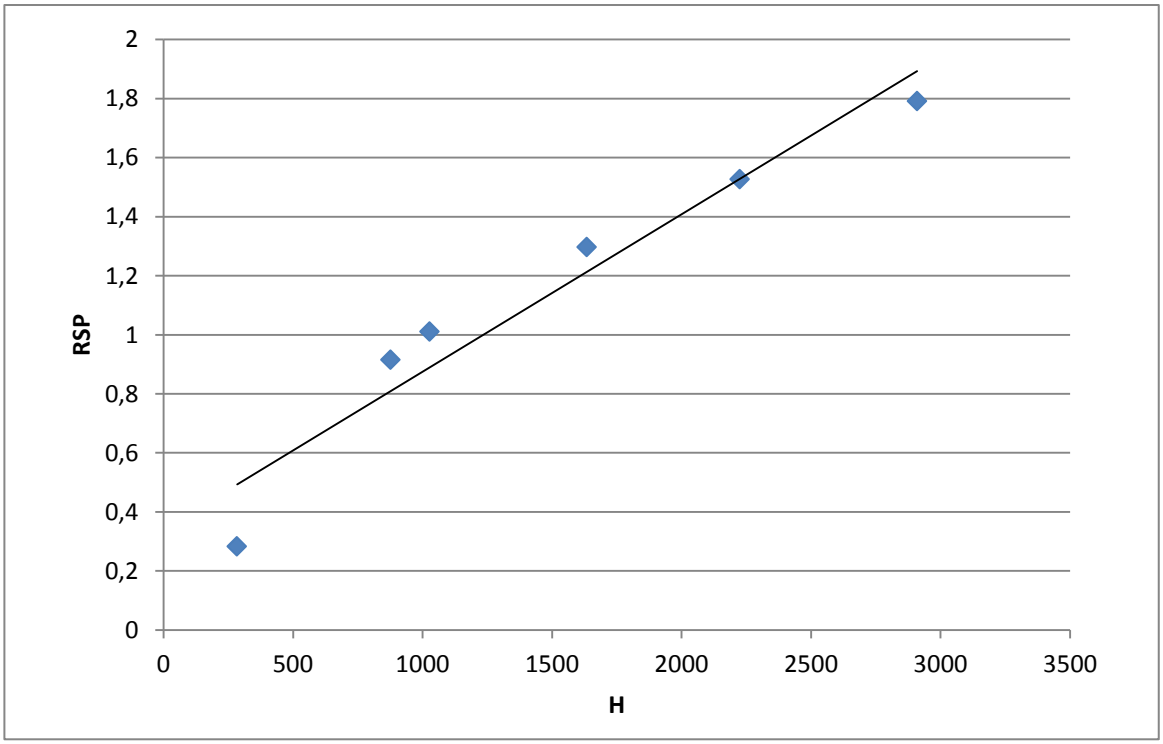

Figure 3: Direct calibration using a linear relation (solid line) fitted to the data points of six calibration materials.

4.2 Evaluation of the direct calibration

The linear calibration curve was compared to the synthetic scaled Hounsfield units and theoretical RSP values of the 81 biological tissues (Figure 4). The relative differences in RSP values were calculated as the difference between the RSP values found with the calibration method and the theoretical values divided by the theoretical RSP values for the tissues. The relative differences were plotted versus their scaled Hounsfield units (Figure 5). From inspection of Figure 5 it can be concluded that the relative differences between RSP values from the calibration and theoretical RSP values were found to be about 15% lower for tissues with scaled Hounsfield units of about 1000 (the scaled Hounsfield units value of water and soft tissues), about 5% lower for tissues with scaled Hounsfield units above 1400 (the scaled Hounsfield units for more dense tissue like bone) and 85% higher for the data point of lung tissue (the one with the lowest scaled Hounsfield units). These differences are quite large. The results show that a linear relation is insufficient to describe the relation between scaled Hounsfield units and RSP values for this range of scaled Hounsfield units. A difference of -15% in the estimation of the RSP value in practice would mean that for tumour at the depth of ten centimetres, you would only give the protons enough energy to go 8.5 centimetres. The proton beam would not reach the distal 1.5 centimetres end of the tumour, which would therefore not receive enough dose. The differences in RSP values from the calibration method and the theoretical values are too large for this calibration method to be used in clinical applications.

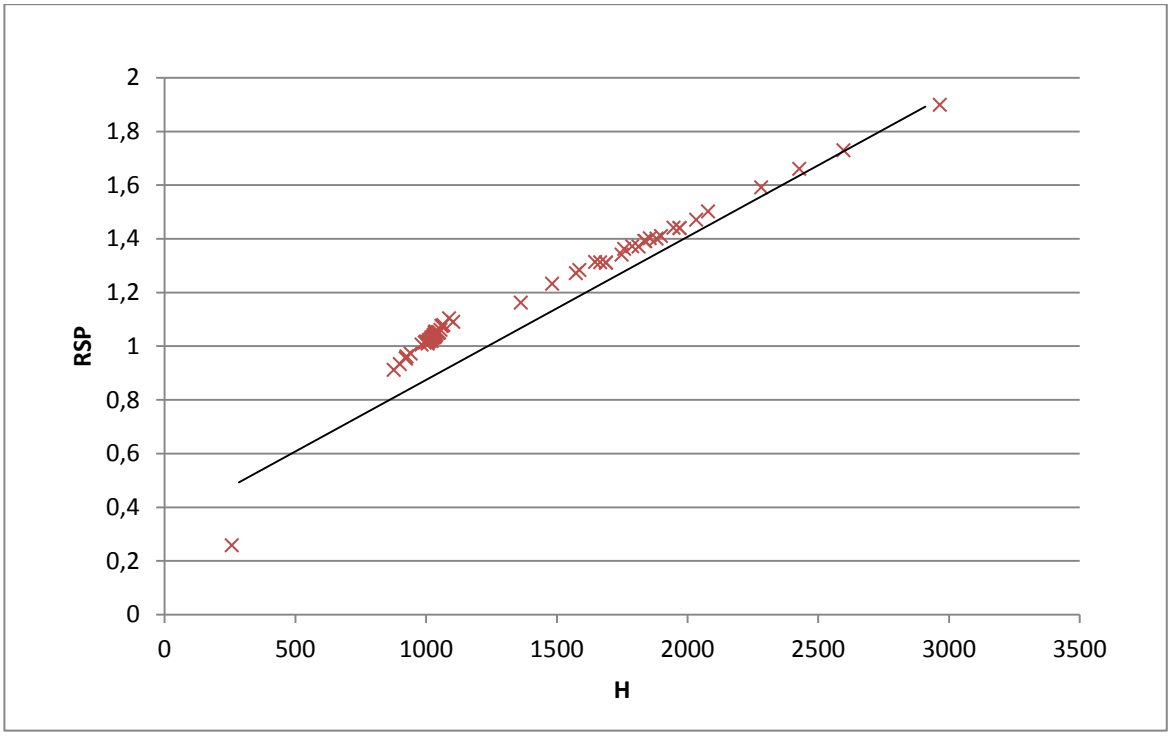

Figure 4: Comparison between the direct calibration curve fit from the six calibration materials (solid line) and theoretical RSP values of 81 biological tissues (red crosses).

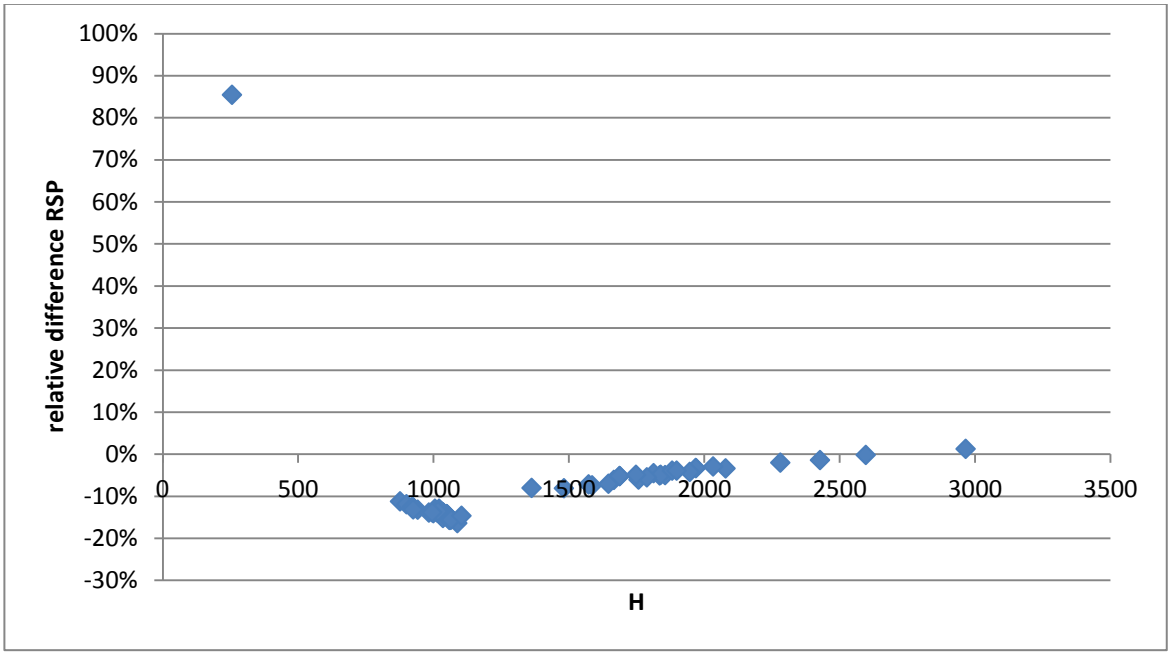

Figure 5: Relative difference between RSP values found with the direct calibration method compared with theoretical RSP values for the 81 biological tissues.

5. The stoichiometric calibration method

The stoichiometric calibration method is more sophisticated than the direct calibration method. In this method the *Z* (atomic number) or elemental composition dependence of the attenuation coefficient is taken into account. Scaled Hounsfield units can be calculated from the ratio of the attenuation coefficient of a compound divided by the attenuation coefficient of water. This way the scaled Hounsfield unit also becomes Z dependent. Constants in the *Z* dependent model for the response of the CT unit in scaled Hounsfield numbers are calibrated using an optimization of the constants, which minimizes the differences between scaled Hounsfield units from the model and scaled Hounsfield units measured by the CT scanner (In our case synthetic scaled Hounsfield units) for the same six calibration materials used for the direct calibration method. With the calibrated model, scaled Hounsfield numbers can be calculated for the 81 biological tissues of which the elemental compositions are known. When the theoretical RSP values are plotted against the modelled scaled Hounsfield unit values for the biological tissues, multiple calibration curves can be fitted to get a more precise calibration between CT scaled Hounsfield units and RSP values.

5.1 The stoichiometric model for scaled Hounsfield units

In the stoichiometric calibration method, a parameterization for the linear attenuation coefficient μ_x is used, in which different processes: (the photoelectric effect, coherent and Compton scattering) contribute to some degree to the attenuation coefficient. The following parameterization for the linear attenuation coefficient for compound x composed of elements i is used [Ja81]:

$$\mu_x = \rho_{e,x}\left(C_{pe}\tilde{Z}^m + C_{coh}\hat{Z}^n + C_{comp}\right) \quad [9]$$

in which $\rho_{e,x}$ is the electron density of compound x, the exponents m and n are usually chosen to be 3.62 and 1.86 respectively [Ru76], $C_{pe,coh,comp}$ are constants relating to the photoelectric effect, coherent and Compton scattering and $\acute{Z}^m$ and $\hat{Z}^n$ are given from the composition by [Ja81]:

$$\tilde{Z}^m = \sum_i \lambda_i Z_i^m \quad [10]$$

and

$$\hat{Z}^n = \sum_i \lambda_i Z_i^n \quad [11]$$

In which λ_i is:

$$\lambda_i = \frac{\omega_i \frac{Z_i}{A_i}}{\left(\sum_i \omega_i \frac{Z_i}{A_i}\right)} \quad [12]$$

The electron density for compound x is calculated using both the mass density and the composition of compound x and is given by [Sc96]:

$$\rho_{e,x} = N_A \rho_x \sum_i \omega_i \frac{Z_i}{A_i} \quad [13]$$

The model makes use of the following relationship between scaled Hounsfield units H and the linear attenuation coefficient:

$$\frac{H}{1000} = \frac{\mu_x}{\mu_{H_2O}} \quad [14]$$

In which μ_x and μ_{H_2O} are the linear attenuation coefficients of compound x and water calculated with equation [9] respectively. Using the parameterized equation for the linear attenuation coefficients the modelled scaled Hounsfield unit becomes [Sc00]:

$$\frac{H}{1000} = \frac{\mu_x}{\mu_{H_2O}} = \frac{\rho_{e,x}\left(C_1 \tilde{Z}_x^m + C_2 \hat{Z}_x^n + 1\right)}{\rho_{e,H_2O}\left(C_1 \tilde{Z}_{H_2O}^m + C_2 \hat{Z}_{H_2O}^n + 1\right)} \quad [15]$$

In this equation C_{comp} has been divided out of the equation to end up with 2 independent constants yet to be determined: $C_1 = C_{pe}/C_{comp}$ and $C_2 = C_{coh}/C_{comp}$.

5.2 Determination of constants C_1 and C_2

To obtain scaled Hounsfield units from the model for all materials with known composition and electron density, first the constants C_1 and C_2 have to be determined. For this a minimisation of the sum of the squared residuals between scaled Hounsfield units calculated with the model and synthetic scaled Hounsfield units was used. This was done for the same six calibration materials which were used for the direct calibration. This method gave values for C_1 and C_2 of $5.70 \cdot 10^{-5}$ and $1.89 \cdot 10^{-3}$ respectively, these values are of the same order as values found by Schneider et al [Sc00] of $3.06 \cdot 10^{-5}$ and $1.24 \cdot 10^{-3}$. The ratio C_2/C_1 of 33.2 is quite near the ratio C_{coh}/C_{pe} of 34.9 found in [Sc96].

A plot was made of the relative difference in scaled Hounsfield units found from the stoichiometric model compared with synthetic Hounsfield units for the six calibration materials (Figure 6). From inspection of Figure 6 it can be concluded that differences between scaled Hounsfield units from the model and synthetic values for the calibration materials are quite small, on the order of 10^{-3}. Furthermore, it can be seen that the data point for LN300, a lung tissue calibration substitute, the one with the lowest scaled Hounsfield unit, is an outlier, but even for this material the difference is only 0.25%.

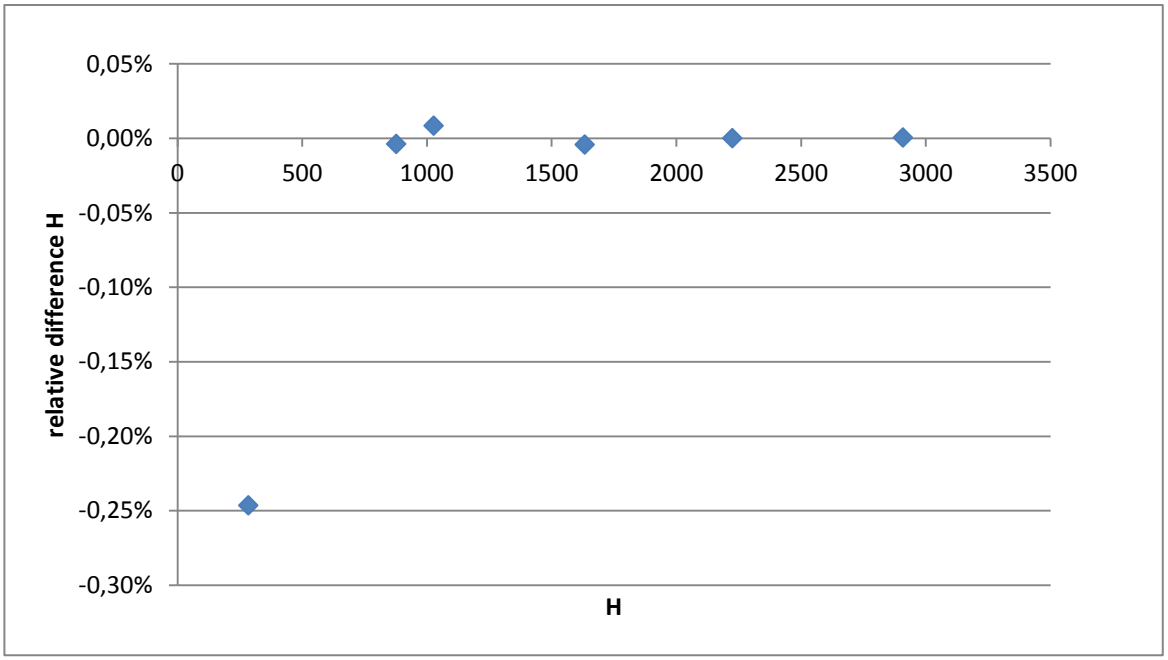

Figure 6: Relative difference between scaled Hounsfield values derived from the stoichiometric model and synthetic scaled Hounsfield values for six calibration materials plotted versus their synthetic scaled Hounsfield units.

Using the calibrated model [equation 15], scaled Hounsfield units were calculated from the composition data of the 81 biological tissues. A plot was made of the relative difference between the scaled Hounsfield units found from the stoichiometric model and synthetic scaled Hounsfield values for the 81 tissues (Figure 7). From inspection of Figure 7 it can be seen that scaled Hounsfield units found from the model differ on average +0.8% for tissues with scaled Hounsfield values of about 1000 and up to almost +3% for tissues with scaled Hounsfield values above 1400. This can be considered a systematic deviation in the scaled Hounsfield values found from the model compared with synthetic values.

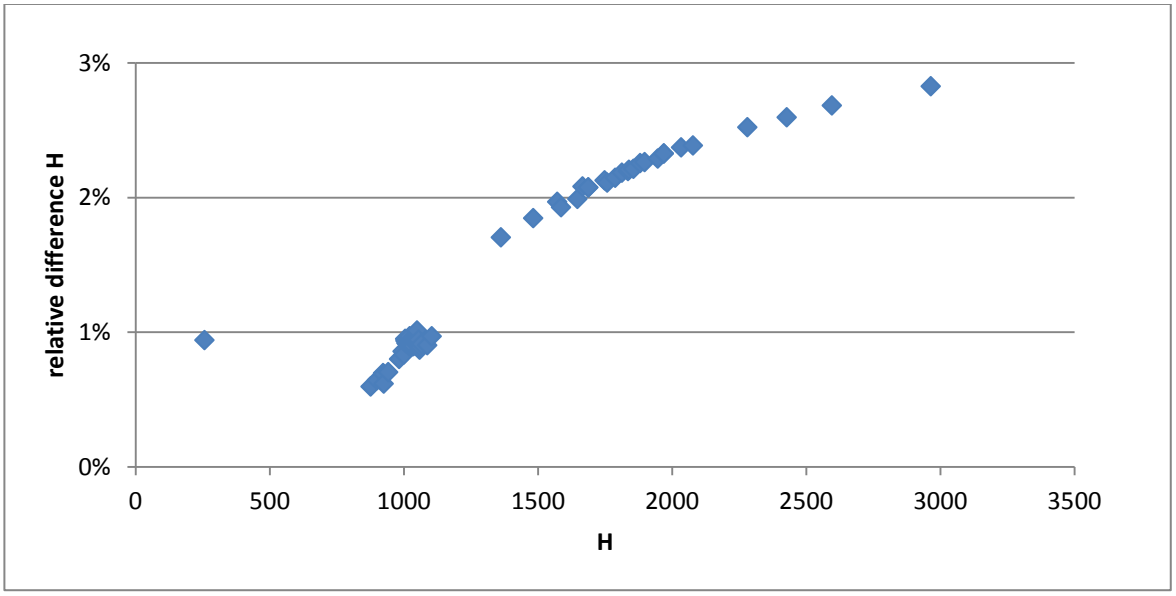

Figure 7: Plot of the relative difference between scaled Hounsfield values found from the stoichiometric model, and the synthetic scaled Hounsfield units of the 81 tissues.

5.3 Stoichiometric calibration curves

To get the calibration curves between CT scaled Hounsfield units and RSP values, the scaled Hounsfield units from the model and theoretical RSP values of the 81 biological tissues are used. A plot was made of RSP values versus scaled Hounsfield units for the 81 biological tissues (Figure 8). In the data set there are two linear regimes at the intervals $882 \leq H \leq 1115$ and at $1385 \leq H \leq 3050$. Furthermore, there are two gaps in the data set where there were only two data points spanning the gap. These gaps occur on the intervals: $259 \leq H < 882$ and $1115 < H < 1385$. To these two gaps and linear regimes four linear relations were fitted, to end up with a calibration between CT Hounsfield units and RSP values. The equation for the linear fits is $\mathrm{RSP} = a\mathrm{H} + b$. The values found for *a* and *b* for the different regimes are given in Table 3. The relative differences between the theoretical RSP values and RSP values found from the linear equations using the scaled Hounsfield values from the stoichiometric model are plotted in Figure 9. The relative differences in RSP values are found to be within $\pm$ 1.5%.

Table 3: Values found for parameters *a* and *b* for the linear relations fitted to the four regimes.

Regime	*a*	*b*
$259 \leq H < 882$	0.001051	0.0144
$882 \leq H \leq 1115$	0.00079	0.217
$1115 < H < 1385$	0.000436	0.7966
$1385 \leq H \leq 3050$	0.000264	0.5681

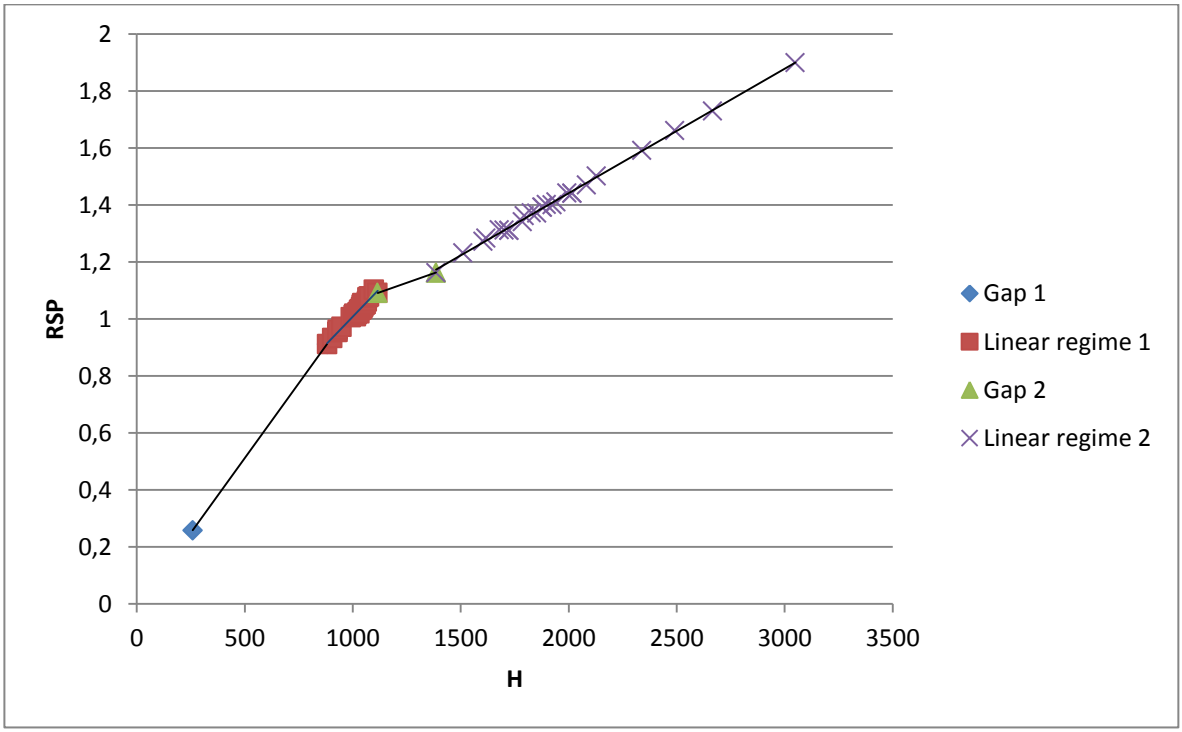

Figure 8: Plot of scaled Hounsfield units from the stoichiometric model versus synthetic RSP values for 81 tissues, with linear relations as calibration curves fitted through the two gaps and two linear regimes.

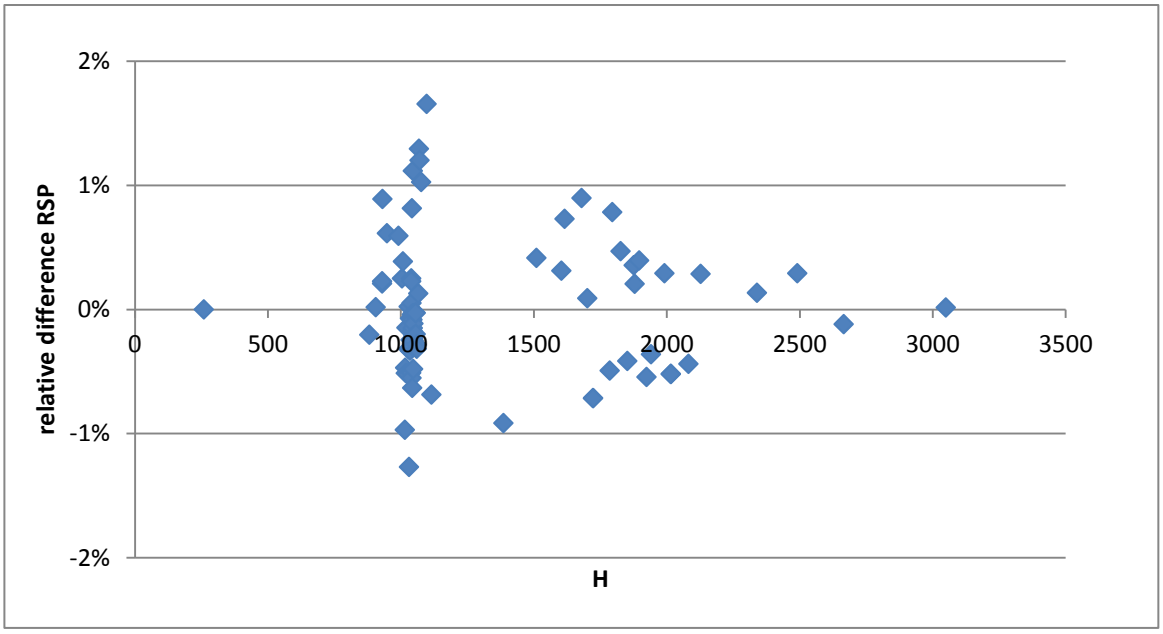

Figure 9: Relative differences in RSP values found from the four linear relation fits compared with RSP values from the model in percentages.

5.4 Evaluation of the stoichiometric calibration.

The stoichiometric calibration method is compared to the synthetic data of the 81 biological tissues by calculating RSP values from the stoichiometric calibration curves using the synthetic Hounsfield units, and comparing them with the theoretical RSP values. To visualize this evaluation, a plot was made of the calibration curves and the synthetic data points (Figure 10). In this plot it can be seen that the calibration curves slightly underestimate the theoretical RSP values of the theoretical data. A plot was made of the relative differences between the RSP values found from the stoichiometric calibration method and the theoretical RSP values, a fourth degree polynomial trend line was fitted to the data and represents the systematic deviation in the results (Figure 11).

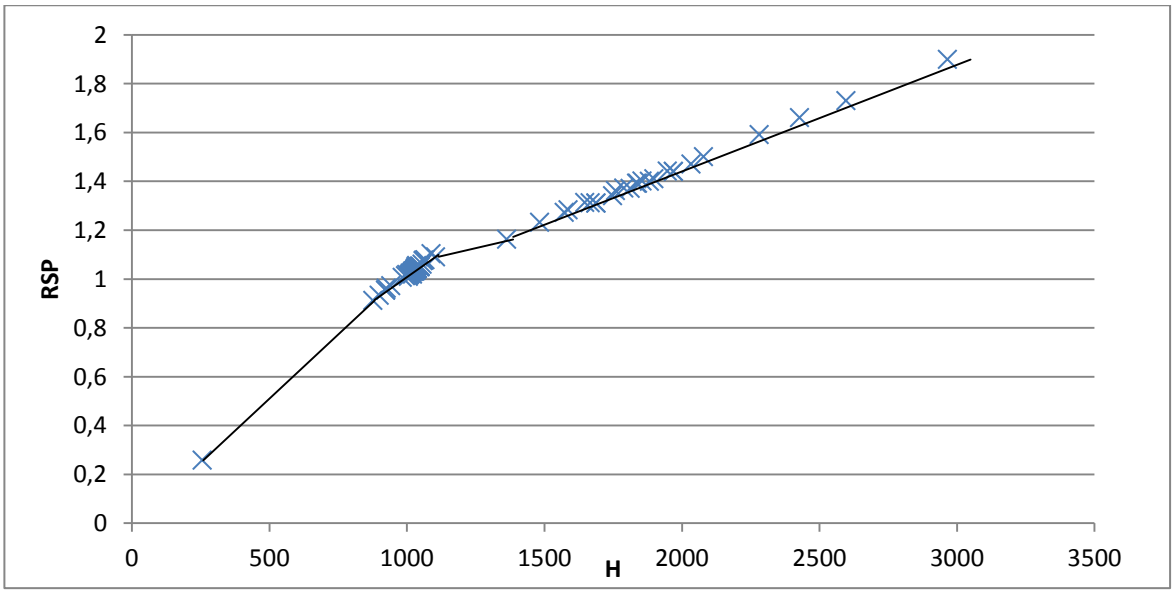

Figure 10: Plot of the synthetic data points of RSP values and scaled Hounsfield units for the 81 tissues and stoichiometric calibration curves for the four different regimes.

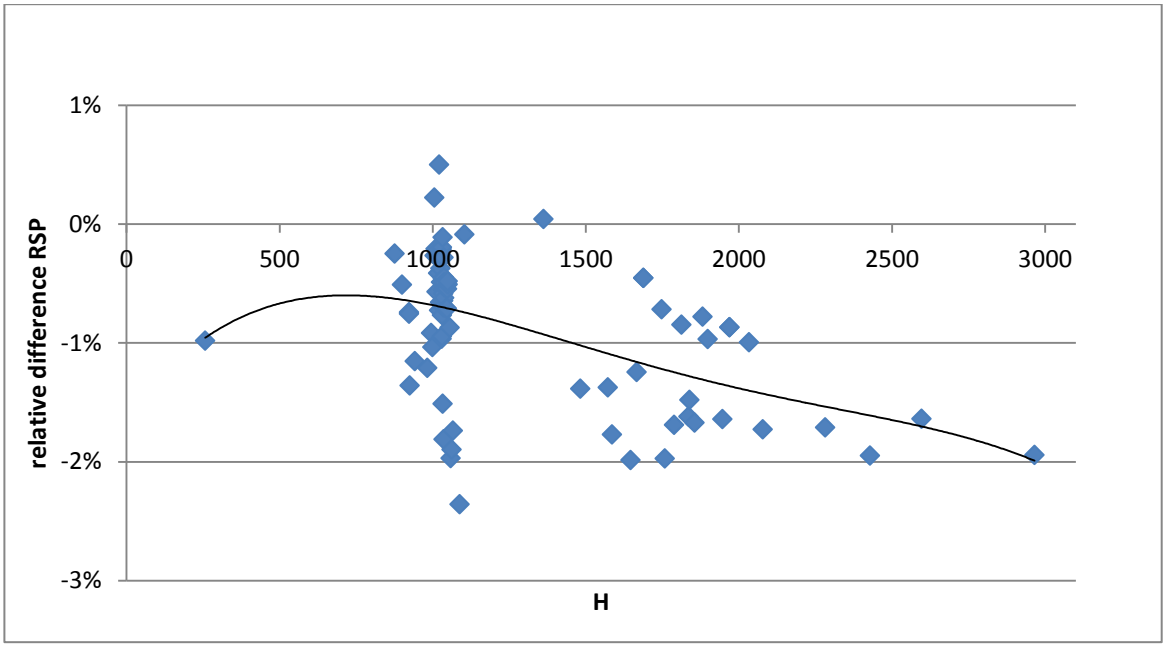

Figure 11: Plot of the relative differences between RSP values found from the stoichiometric calibration method and theoretically found values for the 81 biological tissues. The solid line is a fourth degree polynomial fitted to the data and represents the systematic deviation in the results of the stoichiometric calibration method.

From Figure 11 we observe that, RSP values found from the stoichiometric calibration turned out to be on average about 0.5% lower for tissues with scaled Hounsfield values of about 1000 and from up to 2% lower for tissues with scaled Hounsfield units above 1400 compared with the synthetic RSP values, this can be considered as a systematic deviation. This difference can be explained by the fact that the stoichiometric model overestimates the scaled Hounsfield units for the real tissues. Earlier we found that relative differences in scaled Hounsfield units between values from the stoichiometric model and synthetic values are on the order of +0.8% for tissues with scaled Hounsfield units of about 1000 and up to +3% for tissues with scaled Hounsfield units above 1400 (Figure 7). This causes the use of too high scaled Hounsfield units in creating the calibration curves, which ends up in underestimating RSP values for real CT scaled Hounsfield unit data. Furthermore, the same spread of data points as in Figure 9 can be recognized in Figure 11 (upto 1.5% deviation). This spread results from the linear fitting to data points which deviate up to 1.5%. The 1.5% deviation of the data points is a result of differences in compositions of different tissues.

To improve the stoichiometric calibration method, ideally a better model for the scaled Hounsfield units should be used by either changing the model or the calibration of the model. The calibration of the stoichiometric model can in theory also be done using the 81 biological tissues. When synthetic scaled Hounsfield units and composition data for the 81 tissues are used to do the calibration of C1 and C2, the difference in scaled Hounsfield units from the model compared with the synthetic data becomes $\pm 1\%$ for tissues with scaled Hounsfield units of about 1000 and only $\pm 0.3\%$ for tissues with scaled Hounsfield units above 1400 (Figure 12). From inspection of Figure 12 it can be seen that the relative differences in modelled scaled Hounsfield units in this case are positive as well as negative so the systematic deviation due to the overestimation of the scaled Hounsfield units for the tissues will no longer be there. Unfortunately it is not practical to use CT scaled Hounsfield units and composition data of 81 real

tissues to calibrate the model in practice, because one needs to have 81 real tissues lying around and know their elemental composition. But by carefully picking calibration materials which do have a composition close to the average composition of real tissues, it should be possible to get a better calibration, without systematic deviation. Another option to get a better calibration could be to do measurements of the RSP values for a few materials which span the scaled Hounsfield unit range using the proton beam system. And compare the measured values with RSP values from the calibration method, and then afterwards correct the calibration for the systematic deviation in the calibration.

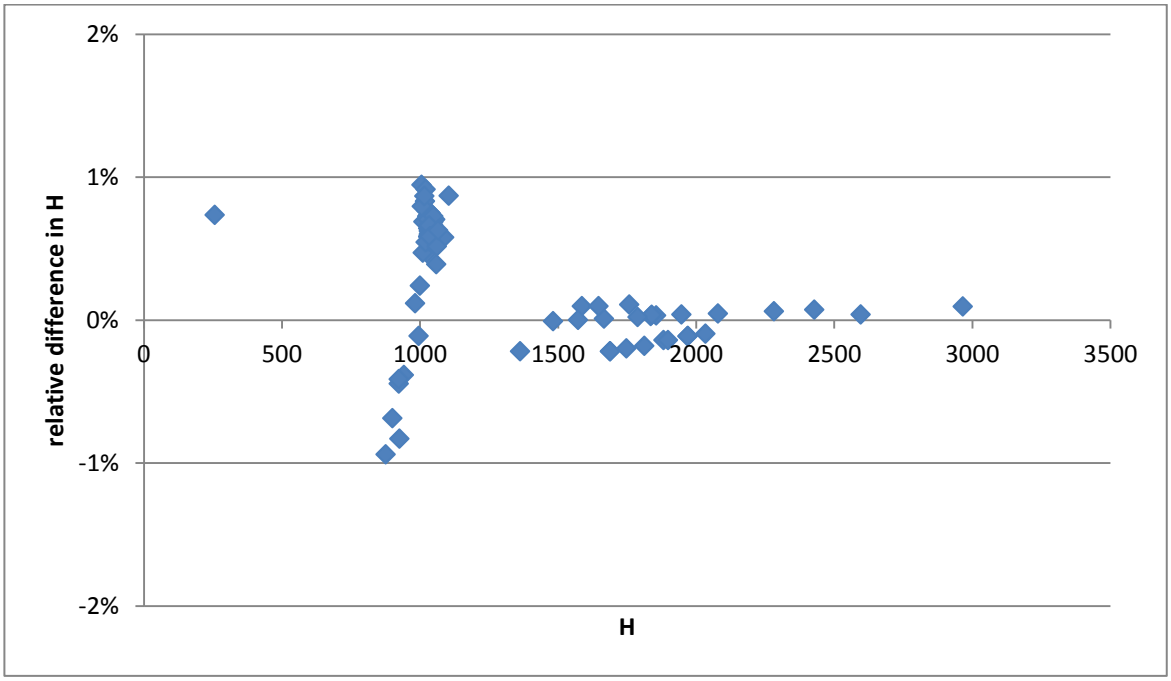

Figure 12: Plot of relative difference between scaled Hounsfield units from the stoichiometric model calibrated using the composition data of the 81 tissues and synthetic scaled Hounsfield units for the 81 tissues.

If perfect calibration materials are chosen, there should be no or at least a much smaller systematic deviation in the RSP values found by the stoichiometric calibration method. To simulate such an outcome, a fourth degree polynomial trend line was fitted to the data in the relative difference in RSP values plot which represents the systematic deviation (Figure 11). The fourth degree polynomial was subtracted from the relative difference in RSP values to get rid of the systematic deviation (Figure 13).

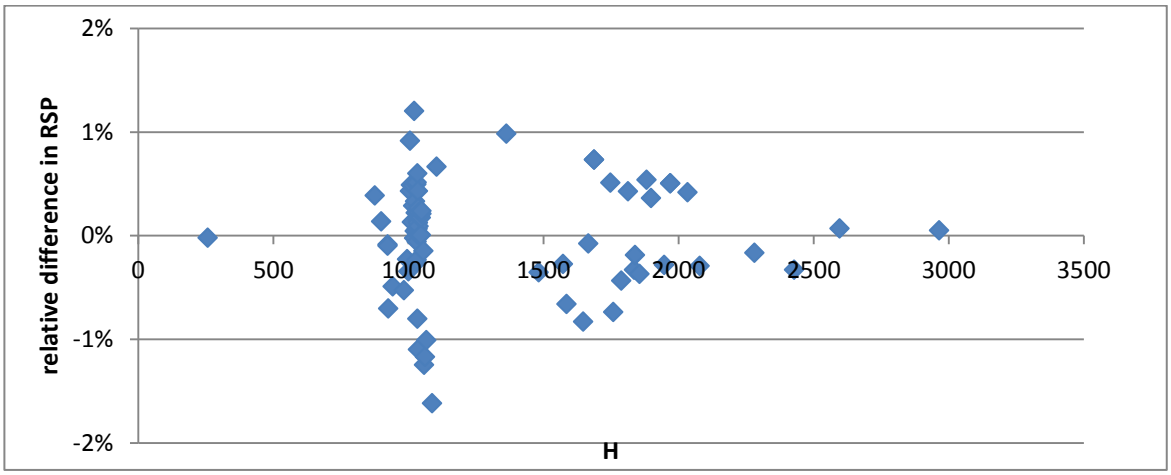

Figure 13: Plot of relative differences in RSP values between values from the stoichiometric calibration method which were corrected for the systematic deviation and theoretical values for the 81 biological tissues.

6. Composition lookup table calibration method (Ray-search method)

A calibration method which is currently commercially used is the calibration method using a composition lookup table. This method is described in Raystation 4.5 reference manual [Ra14]. For this calibration method, the CT commissioner creates a table of CT measurements for about 15 tissue equivalent calibration materials with known density, which are equally spread along the Hounsfield unit scale from air to solid bone (in our case again synthetic Hounsfield units are used for this). This table is called the CT-to-density-table. In this table, densities for CT measured Hounsfield values are interpolated. The composition lookup table is a table with composition, density and mean ionization potential data for 56 materials. The interpolated densities are linked to one of 56 different material compositions and mean ionization potentials from a composition lookup table. This is done by searching for the material in the composition lookup table which has the density which is the closest to the interpolated density. The data for the 56 different materials has been interpolated from 10 ''core materials'' which are expected to be found in the human body and of which the density, composition and mean ionization potential is known. From the interpolated density, and the composition and ionization potential from the composition lookup table, RSP values are calculated using the algorithms unknown to us in RayStation 4.5, in this report equations 4,5,6,7 and 8 are used for this.

6.1 Creating the CT-to-density-table and performing the interpolation.

The CT-to-density-table is made by the CT-commissioner and should represent the whole scaled Hounsfield unit range from air to solid bone. In this report densities and synthetic Hounsfield units for the materials in Table 4 are used for this purpose.

Table 4: CT-to-density-table containing 15 tissue equivalent materials and their corresponding densities and scaled Hounsfield units.

Material	ρ (g cm^{-3})	H
AIR	0.00	1
LN300	0.29	284
LN450	0.43	419
AP6	0.95	877
BR12	0.98	932
BRN-SR2	1.05	986
CT SW	1.01	996
water	1.00	1000
SW M457	1.05	1027
LV1	1.10	1077
IB3	1.15	1366
B200	1.16	1374
CB2-30%	1.33	1634
CB2-50%	1.56	2226
SB3	1.82	2910

There are three linear regimes within this table. To do interpolation within the table, three linear relations were fitted to the linear regimes: (0<H<877),(877<H<1076) and (1076<H<3000)(Figure 14). The equation for the linear relations is: $\rho = a\mathrm{H} + b$ in which ρ is the interpolated mass density and a and b for the different regimes are given in Table 5.

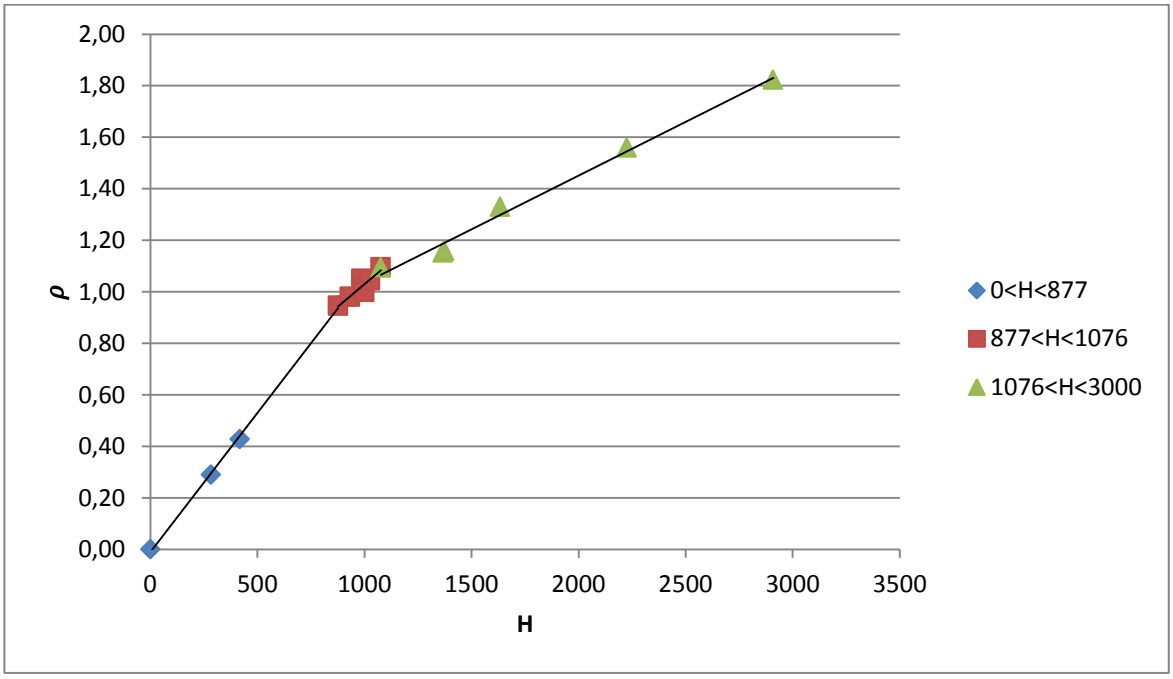

Figure 14: Plot of density vs scaled Hounsfield units for 15 calibration materials, with three linear relations fitted to the linear regimes as calibration curves (solid lines).

Table 5: Values found for parameters *a* and *b* for the linear relations fitted to the three linear regimes.

Regime	***a***	***b***
0<H<877	0.001082	-0.01119
877<H<1076	0.0007061	0.3234
1076<H<3000	0.0004170	0.6177

6.2 Composition lookup table.

The composition lookup table is a list of 56 materials, with information about the composition and mean ionization potential of these materials. It is made by interpolation of the composition and ionization potentials of 10 ''core materials'' that are expected to be found in the patient. The materials are interpolated with respect to their mass density. For a material C interpolated between the core materials $A(\rho^a, \omega(Z)^a, I^a)$ and $B(\rho^b, \omega(Z)^b, I^b)$ the elemental composition $\omega(Z)^c$ and the mean ionization potential I^C are calculated as [Ra14]:

$$\omega(Z)^c = \omega^a \omega(Z)^c + \omega^b \omega(Z)^c \quad [16]$$

$$\ln I^c = \frac{\omega^a (Z/A)^a ln I^a + \omega^b (Z/A)^b ln I^b}{(Z/A)^c} \quad [17]$$

in which:
$(Z/A)^x = \sum_i \omega(Z_i)^x \frac{Z_i}{A_i}$: the number of electrons to molecular weight ratio of material x composed of elements i;
$\omega^a = \frac{f^a \rho^a}{\rho^c}$, $\omega^b = \frac{f^b \rho^b}{\rho^b}$: the weights for material *A* and *B* and in which:
$f^a = \frac{V^a}{V^a + V^b} = \frac{\rho^b - \rho^c}{\rho^b - \rho^a}$, $f^b = 1 - f^a$: the relative volume fractions and in which: V^a and V^b are the relative volumes and ρ^a and ρ^b the mass densities of materials *A* and *B.* In this report a finished composition lookup table from ray-search was used [Tr16].

6.3 Retrieving RSP values from the composition lookup table calibration method.

When the CT-to-density-table and the composition lookup table are made, RSP values can be retrieved for all CT data. First, densities are linked to the CT data using the linear interpolation relations in the CT-to-density table. Then the densities must be linked to the composition of one of the 56 materials in the composition lookup table, which has the density which is the closest to the interpolated density. This was done by searching for which material occurred the minimum in a list of the squared differences between the interpolated densities and the density of the 56 different materials from the composition lookup table. The RSP values are then calculated using the interpolated density, and the composition and ionization potential from the material from composition lookup table, which was linked to the interpolated density using equations [4,5,6,7 and 8]. This procedure was done for the synthetic scaled Hounsfield unit data for the 81 biological tissues. A plot was made of the relative differences between the interpolated densities and densities from the composition data of the 81 tissues (Figure 15). From inspection of Figure 15, it can be concluded that relative differences between the interpolated densities and densities from the composition data of the 81 tissues are found to be within $\pm$2.3% for tissues with scaled Hounsfield units of about 1000 and within $\pm$0.8% for tissues with scaled Hounsfield units above 1400.Furthemore, there is a systematic deviation, for lung tissue, the tissue with the lowest scaled Hounsfield unit, the estimated density is almost 3% to large. The data points with scaled Hounsfield units above 1400 have densities which are underestimated by up to 3%. The density of connective tissue is largely underestimated with about 4.3% this is due to the fact that the

density is interpolated using the calibration curve for bone tissues but has a composition more comparable to soft tissues.

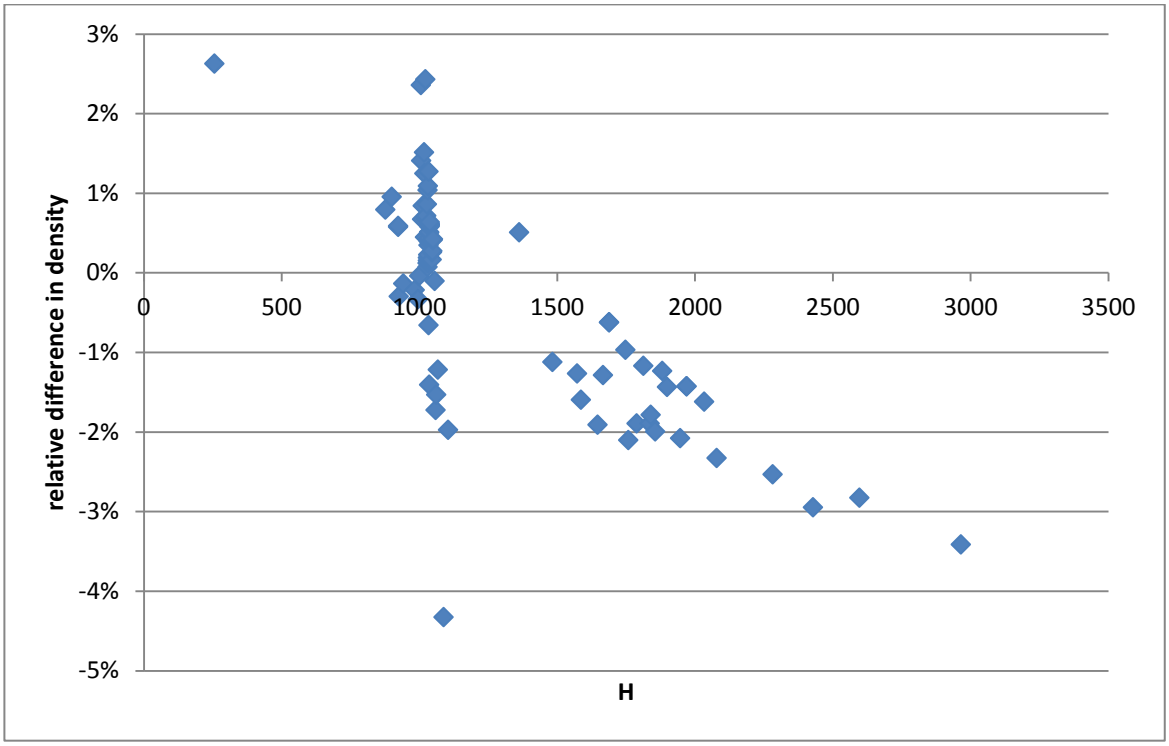

Figure 15: Plot of relative differences between interpolated densities and densities from the composition data for the 81 biological tissues.

6.4 Evaluation of the lookup table calibration method

A plot was made of the relative difference between the RSP values found from the composition lookup table calibration method and the theoretical RSP values for the 81 tissues (Figure 16). From comparison of Figure 15 and 16 it can be concluded that the relative differences in RSP values and densities have about the same spread and systematic deviation. The largest difference is that the data points for the relative difference in RSP values are about 1% more positive. From these results it can be concluded that the mean ionization potential and composition data from the lookup table do not contribute a lot to the precision of this calibration method. The systematic deviation which appears in the results is caused by the systematic deviation in the calibration between scaled Hounsfield units and densities, the cause of this systematic deviation is that the 15 calibration materials used in the CT-to-density-table have too high density for the calibration materials with scaled Hounsfield unit below 500 and too low densities for the calibration materials above scaled Hounsfield units of 1500 compared with the densities of the 81 tissues. To improve the CT-to-density calibration and get rid of the systematic deviation, other calibration materials should be chosen, which have scaled Hounsfield unit values and densities which are more comparable with those of real tissues. The $\pm$2% spread in relative difference in RSP values around the scaled Hounsfield unit of 1000 is a result of fitting a linear relation to data points with this $\pm$2% spread and cannot be overcome in this calibration method.

Again, if perfect calibration materials are chosen, there should be no systematic deviation in the RSP values found by the composition lookup table calibration method. To simulate such an outcome, a fourth degree polynomial trend line was fitted to the data in the relative difference in

RSP plot which represents the systematic deviation (Figure 16). The fourth degree polynomial was subtracted from the relative difference in RSP values to minimize the systematic deviation (Figure 17).

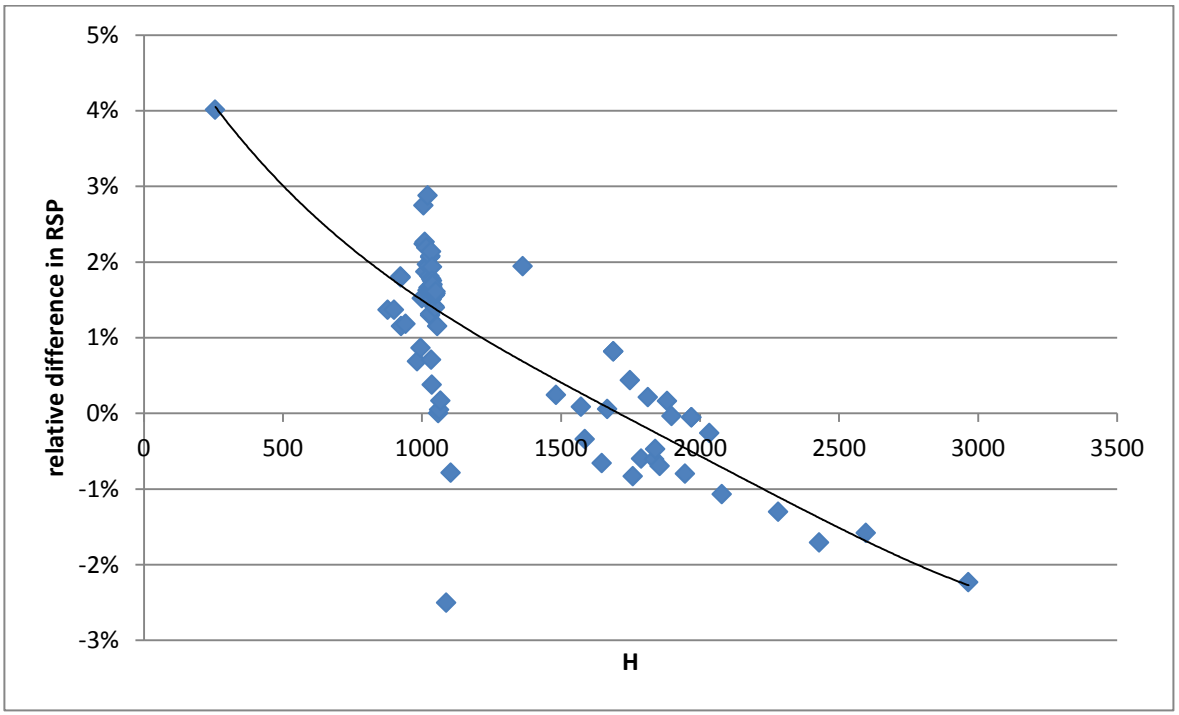

Figure 16: Plot of the relative difference between RSP values from the lookup table calibration method and the theoretical values for the 81 tissues. The solid line is a fourth degree polynomial fitted to the data and represents the systematic deviation in the results of the lookup table calibration method.

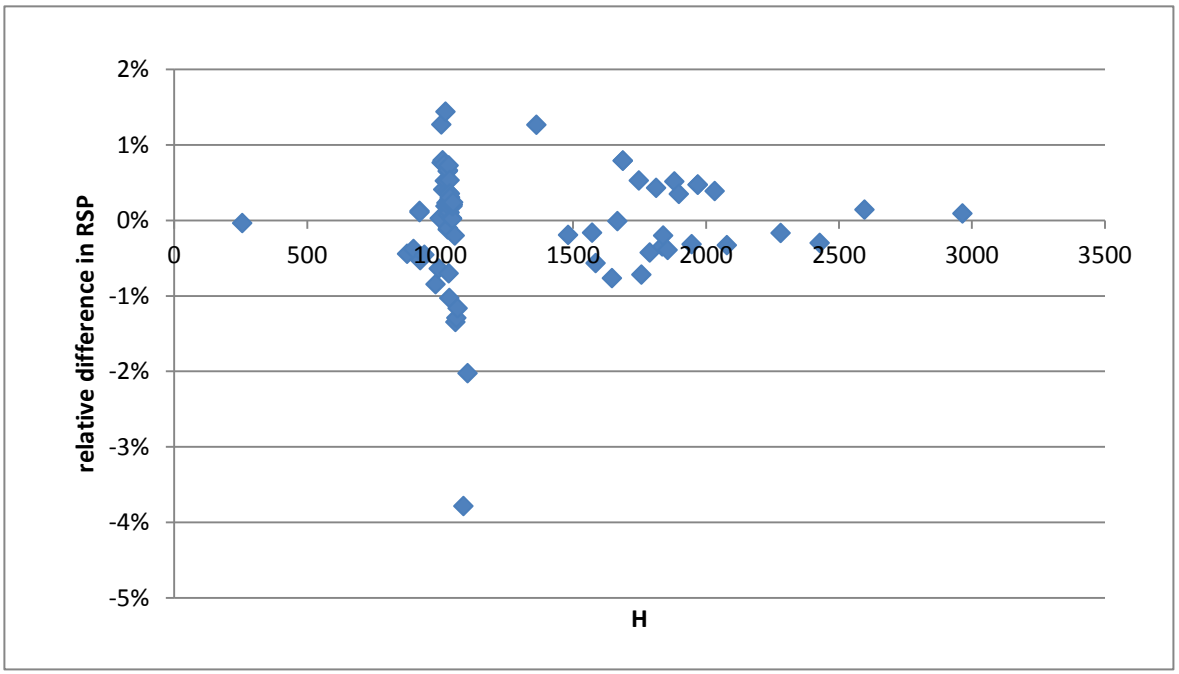

Figure 17: Plot of relative differences in RSP values between values from calibration method using a composition lookup table which were corrected for the systematic deviation and theoretical values for the 81 tissues.

7. Comparison of the direct, stoichiometric and composition lookup table calibration methods.

In this report we considered three different SECT calibration methods convert CT Hounsfield units to RSP values for protons in biological tissues: the direct, stoichiometric and composition lookup table calibration method. From the results it can be concluded that the direct calibration method does not do a good enough job at estimating RSP values to be used in clinical practice, with relative differences of about -15% for tissues with scaled Hounsfield units of about 1000, of about -5% for tissues with scaled Hounsfield units of above 1300 and +85% for lung tissue.

The stoichiometric calibration method and the composition lookup table calibration method are more accurate in estimating RSP values. Our analysis showed that both calibration methods had a systematic deviation, which was due to the fact that the calibration materials did not have the same average compositions and densities, and therefore the same average RSP values as the real tissues. The standard deviation for the relative differences in RSP values for both the results of the calibration methods corrected for the systematic deviation and not corrected are given in Table 6. Furthermore, the maximum absolute deviation and range of the systematic deviation are also given. The standard deviations for the uncorrected and corrected results and the maximum absolute deviation are all lower for the stoichiometric calibration method. This indicates that the stoichiometric calibration method gives more accurate values for RSP values for different tissues. The range of the systematic deviation is smaller for the stoichiometric calibration method, indicating that this calibration method is less sensitive to composition and density differences between the calibration materials and the real tissues.

Table 6: Standard deviations in the relative difference in RSP values for both the results which were corrected and not corrected for the systematic deviation for the stoichiometric calibration method and composition lookup table calibration method. The maximum absolute deviation and range of the systematic deviation in the relative difference in the RSP values is also given.

Calibration method	RMS deviation for uncorrected results (%)	RMS deviation for corrected results (%)	Maximum absolute deviation (%)	Range RSP systematic deviation (%)
Stoichiometric	1.39	0.59	1.6	-0.5 to -2
Composition lookup table	1.62	0.81	3.8	4 to -2

Furthermore, in the composition lookup table calibration method 15 calibration materials, which are evenly spread along the scaled Hounsfield unit scale, were needed to get a precise relation between CT data and interpolated density. In the stoichiometric calibration method only 6 calibration materials were used. This gives a practical advantage to the stoichiometric calibration method.

Acknowledgements

I would like to express my appreciation to E.R. van der Graaf for his guidance in this Bachelors project. Furthermore, I would like to thank E.R. van der Graaf and A.K. Biegun for careful reading of the report.

References

[Ab16] J.K. van Abbema, M-J van Goethem, J. Mulder, A.K. Biegun, G.J. Pelgrim, M. Vonder, M. J. W. Greuter, A. van der Schaaf, S. Brandenburg, E. R. van der Graaf, Prediction and experimental validation of proton stopping powers from DECT, submitted to Physics in Medicine and Biology, July 2016.

[Ai14] C.G. Ainsley, C.M. Yeager, *Practical considerations in the calibration of CT scanners for proton therapy.* Journal of Applied Clinical Medical Physics 16, 202-220, 2014

[Ci16] Cijfers over kanker Website: http://www.cijfersoverkanker.nl/incidentie-sterfte-50.html, 2016.

[Ja81] D.F. Jackson and D.J. Hawkes, *X-ray attenuation coefficients of elements and mixtures.*Phys. Rep. 70 169-233, 1981.

[Ni15] NIST Website: http://www.nist.gov/pml/data/comp.cfm, 2015.

[Ni16] NIST website: http://physics.nist.gov/cgi-bin/Star/compos.pl?matno=104, 2016.

[Pa12] H. Paul, *The stopping power of matter for positive ions.*Modern practice in radiation therapy, chapter 7, 113-132, 2012.

[Pe16] E. Pedroni, *advantages of protons over photons,* website: http://sunse.jinr.ru/~molod/concept/adv-protons.html, 2016.

[PT16] HollandPTC website: http://www.hollandptc.nl/nederlands/protonentherapie/, 2016.

[Ra14] RSL-D-61-218-REF-EN-2.0-2014-07-01 RAYSTATION 4.5 REFERENCE MANUAL, Chapter 2, 19-30, 2014.

[Ru76] R.A. Rutherford, B.R. Pullan, I. Isherwood, Measurements of effective atomic number and electron density using an EMI scanner. Neuroradiology 11, 15-21, 1976.

[Sc96] U. Schneider, E. Pedroni, A. Lomax, *The calibration of CT Hounsfield units for radiotherapy treatment planning.* Phys. Med. Biol. 41, 111-24, 1996.

[Sc00] W. Schneider, T. Borfeld, W. Schlegel, *Correlation between CT numbers and tissue parameters needed for Monte Carlo simulations of clinical dose distribution.* Phys. Med. Biol. 45, 459-78, 2000.

[Si16] Courtesy of Siemens Medical Solutions, Forchheim, Germany, 2016

[Tr16] Erik Traneys, Raysearch, personal communication, May 2016.

[Tu07] J.E. Turner, *Atoms, radiation, and radiation protection.* Wiley,2007.

[Wh87] D.R. White, H.Q. Woodard, S.M. Hammond, Average soft-tissue and bone models for use in radiation dosimetry, Br. J. Radiol. 60, 907–913, 1987

[Ya12] M. Yang, X.R. Zhu,P.C.Park, U. Titt, R. Mohan, G. Vishup, J. Clayton, L.Dong, *Comprehensive analysis of proton range uncertainties related to patient stoppingpower-ratio estimation using the stoichiometric calibration.* Phys. Med. Biol. 57, 4095-4115, 2012.